AVP2, a Sequence-Divergent, K^+-Insensitive H^+-Translocating Inorganic Pyrophosphatase from Arabidopsis[1]

Yolanda M. Drozdowicz, Jessica C. Kissinger, and Philip A. Rea*

Plant Science Institute, Department of Biology, University of Pennsylvania, Philadelphia, Pennsylvania 19104–6018

Plant vacuolar H^+-translocating inorganic pyrophosphatases (V-PPases; EC 3.6.1.1) have been considered to constitute a family of functionally and structurally monotonous intrinsic membrane proteins. Typified by AVP1 (V. Sarafian, Y. Kim, R.J. Poole, P.A. Rea [1992] Proc Natl Acad Sci USA 89: 1775–1779) from Arabidopsis, all characterized plant V-PPases share greater than 84% sequence identity and catalyze K^+-stimulated H^+ translocation. Here we describe the molecular and biochemical characterization of AVP2 (accession no. AF182813), a sequence-divergent (36% identical) K^+-insensitive, Ca^{2+}-hypersensitive V-PPase active in both inorganic pyrophosphate hydrolysis and H^+ translocation. The differences between AVP2 and AVP1 provide the first indication that plant V-PPases from the same organism fall into two distinct categories. Phylogenetic analyses of these and other V-PPase sequences extend this principle by showing that AVP2, rather than being an isoform of AVP1, is but one representative of a novel category of AVP2-like (type II) V-PPases that coexist with AVP1-like (type I) V-PPases not only in plants, but also in apicomplexan protists such as the malarial parasite *Plasmodium falciparum*.

A distinguishing feature of the vacuolar membrane of plant cells is its possession of a vacuolar H^+-translocating inorganic pyrophosphatase (V-PPase; EC 3.6.1.1) as well as a more conventional H^+-ATPase (V-ATPase; EC 3.6.1.3; Rea and Poole, 1993; Zhen et al., 1997a). Both enzymes catalyze electrogenic H^+ translocation from the cytosol into the vacuole, but V-PPase has the unusual characteristic of being energized by PPi instead of ATP.

The plant V-PPase is one of several membrane-associated PPases identified to date. Others include the H^+-translocating PPi synthase on the energy-coupling membranes of the phototrophic purple nonsulfur bacterium *Rhodospirillum rubrum* (Baltscheffsky, 1996), and the PPase activities described for plant submitochondrial particles (SMPs) (Vianello et al., 1991) and thylakoid membranes (Jiang et al., 1997). Of these, the most thoroughly investigated are the plant V-PPase and the bacterial H^+-PPi synthase.

All characterized plant V-PPases have a near obligatory requirement for millimolar concentrations of cytosolic K^+ for activity (Davies et al., 1991), appear to operate predominantly in a hydrolytic mode—pumping H^+ at the expense of PPi—and are considered to contribute to the establishment of the transmembrane H^+-electrochemical potential difference required for the secondary transport of a broad range of solutes in and out of the vacuole (Rea and Poole, 1993; Zhen et al., 1997a). Phototrophic bacterial H^+-PPi synthases are, by comparison, relatively insensitive to monovalent inorganic cations, freely reversible, and considered to be responsible for the maintenance of H^+ gradients—when irradiance is insufficient to sustain direct H^+-coupled ATP synthesis—through the utilization of photosynthetically derived cellular PPi reserves (Nyren and Strid, 1991; Baltscheffsky, 1996). Although it has been suspected for some time from the results of functional studies (Rea and Poole, 1993) that the plant and bacterial enzymes belong to the same class of pumps—a class of H^+-phosphohydrolase distinct from F_1F_0-type, plasma membrane-type, and vacuolar-type ATPases (F-, P-, and V-ATPases, respectively) (Rea et al., 1992b)—the precise structural relationship between these and the PPase activities associated with the membranes of mitochondria and chloroplasts has resisted definition.

While H^+-PPases, specifically V-PPases, had formerly been thought to be restricted to plants and their algal antecedents and subject to pronounced

[1] This work was supported by the Department of Energy (grant no. DE–FG02–91ER20055 to P.A.R.). Y.M.D. is a Triagency (Department of Energy/National Science Foundation/U.S. Department of Agriculture) Plant Training Grant Fellow. Sequencing of the *Chlorobium tepidum* and *Caulobacter crescentus* genomes by The Institute for Genomic Research was accomplished with support from the Department of Energy. Partial sequencing of the *P. falciparum* genome was accomplished by The Institute for Genomic Research, The Sanger Centre, and the Stanford DNA Sequencing and Technology Center as part of the Malaria Genome Project with support from the National Institute of Allergy and Infectious Diseases, National Institutes of Health, The Wellcome Trust, and The Burroughs Wellcome Fund.

* Corresponding author; e-mail parea@sas.upenn.edu; fax 215–898–8780.

sequence conservation (Zhen et al., 1997a), recent developments have shown this not to be the case, and have prompted a renewed interest in this class of pump. Most germane of these new findings are: (a) The molecular cloning of a homolog of the prototypical V-PPase, AVP1 (Arabidopsis vacuolar pyrophosphatase; Sarafian et al., 1992), from *R. rubrum* (RVP; Baltscheffsky et al., 1998). Sequence comparisons between RVP, AVP1, and other plant V-PPases confirm that the plant and phototrophic bacterial enzymes belong to the same class of pumps. From these investigations and those of heterologously expressed (Kim et al., 1994a) and reconstituted (Britten et al., 1992; Sato et al., 1994) V-PPases, it is now evident that these pumps consist of a single 75- to 81-kD intrinsic membrane protein that alone is sufficient for PPi (Mg_2PPi) hydrolysis and H^+ translocation (Zhen et al., 1997a). (b) The isolation, sequence determination, and functional characterization of PVP, a sequence-divergent and thermostable V-PPase ortholog from the facultatively aerobic archaeon *Pyrobaculum aerophilum* (Drozdowicz et al., 1999). The discovery of PVP not only establishes firm criteria for the identification of sequence motifs likely to be critical for PPi-energized H^+ translocation, but also indicates that V-PPases and PPi-energized H^+ translocation are far more deeply rooted phylogenetically than was thought previously (Drozdowicz et al., 1999). (c) The demonstration of plant-like V-PPase genes and/or functionalities in the parasitic protists *Trypanosoma cruzii* (Scott et al., 1998), *Leishmania donovani* (Rodrigues et al., 1999), *Plasmodium falciparum* (GenBank accession no. AAD17215), and *Toxoplasma gondii* (Y.M. Drozdowicz, B. Striepen, D.S. Roos, and P.A. Rea, unpublished data). The existence of V-PPases in parasitic protists, whose animal hosts lack the enzyme (Rea and Poole, 1993), has given rise to the exciting possibility that a better understanding of the mechanism of action and physiological function of this class of pump might spawn new technologies for combating such widespread and debilitating diseases as malaria, toxoplasmosis, and Chagas' disease (Scott et al., 1998).

We extend this new appreciation of the diversity and functional heterogeneity of V-PPases by describing the cloning and functional expression in yeast of a novel, sequence-divergent, K^+-insensitive, H^+-translocating V-PPase, AVP2, from Arabidopsis. The characteristics of AVP2, when compared directly with those of AVP1, clearly demonstrate that even within the same organism V-PPases fall into disparate functional and structural classes. As would be expected if this phenomenon were of general applicability and not restricted to plants, the results of genomic database searches indicate the coexistence of AVP1-like and AVP2-like (type I and II) V-PPases in another phylum of V-PPase-containing eukaryotes, apicomplexan protists.

RESULTS

Isolation of *AVP2*

The genomic sequence of a gene (GenBank accession no. AC005679) capable of encoding a V-PPase homolog was found as a result of BLAST searches of the Arabidopsis database with sequences corresponding to the regions of AVP1, RVP, and PVP exhibiting greatest conservation (positions 248–295, 504–520, 691–702, and 720–732 of AVP1; Drozdowicz et al., 1999). An expressed sequence tag (accession no. ATTS5194–5) corresponding to this gene but lacking the first 267 bp of coding sequence was also found in these searches, suggesting that the gene concerned was transcriptionally active. Accordingly, reverse transcription-PCR of Arabidopsis leaf total RNA using oligonucleotide primers designed to prime a product spanning the entire open reading frame of this gene yielded a 2,403-bp product encoding an 800-amino acid (81-kD) polypeptide, AVP2, sharing 36% sequence identity (51% similarity) with AVP1 (Sarafian et al., 1992; Fig. 1), 38% identity (53% similarity) with RVP (Baltscheffsky et al., 1998), and 43% identity (57% similarity) with PVP (Drozdowicz et al., 1999).

Sequence Characteristics

Several features of AVP2 were striking. First, unlike all previously published plant V-PPase sequences, which share identities of 80% or more throughout their lengths whether they are from different organisms or isoforms from the same organism, the identities between AVP2 and AVP1 were restricted to only limited stretches of sequence (Fig. 1).

Second, parallel application of hydrophobic moment analysis (von Heijne, 1992), the positive-inside rule (von Heijne, 1986), and the charge-difference rule (Hartmann et al., 1989) using the TopPred II program (Claros and von Heijne, 1994) predicted an overall topology for AVP2 similar to that predicted for AVP1 (Zhen et al., 1997b), except for an additional putative transmembrane span encompassing residues 63 to 83 (Fig. 1). If the assignment of a span at this position is correct, AVP2, unlike AVP1, possesses an extremely hydrophilic, cytosolically oriented N terminus.

Third, as would be predicted for a polytopic membrane protein requiring high-stringency interactions with cytosolic ligands, the sequences exhibiting greatest similarity between AVP2 and other V-PPases were those located in putative hydrophilic loops with a cytosolic disposition (Fig. 1). The cytosolic loops of AVP2 and AVP1 had an aggregate similarity of 56%, whereas the extracytosolic loops had an aggregate similarity of only 24%. Of the eight cytosolic loops, loops III and VIII were the most conserved between AVP2 and AVP1, exhibiting sequence identities of 82% and 77%, respectively (Fig. 1).

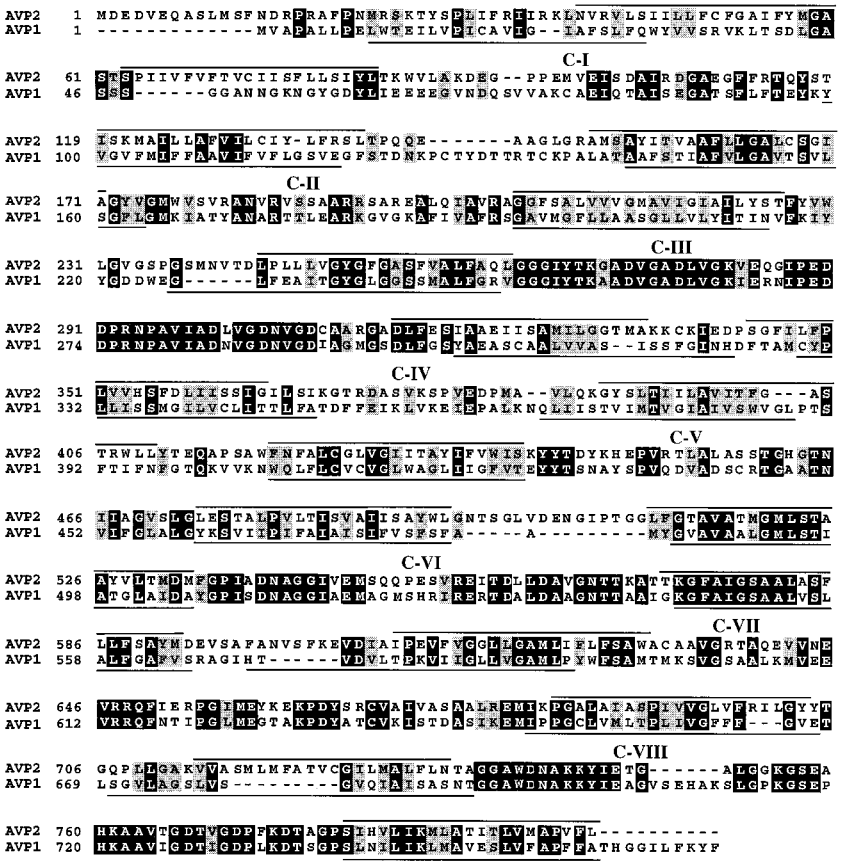

Figure 1. Alignment of AVP2 with AVP1. Residues that are identical between AVP2 and AVP1 are shown in white on a black background. Residues that are similar are shown in black on a gray background. Residues within predicted transmembrane spans are underlined. Residues within cytosolic loops I through VIII are denoted C-I through C-VIII. Sequences were aligned using ClustalW 1.7 (Thompson et al., 1994) and topology was predicted using TopPred II version 1.3 (Claros and von Heijne, 1994).

Fourth, despite its marked divergence from AVP1, AVP2 contained (with one exception) most of the sequence motifs speculated or demonstrated to be necessary for catalysis by plant V-PPases. It contained the putative catalytic motif DX_7KXE, which is found in both soluble and membrane-associated PPases (Rea et al., 1992b); both of the acidic residues (Glu-323 and Asp-532 in AVP2; Glu-305 and Asp-504 in AVP1) that contribute to susceptibility to inhibition by *N,N′*-dicyclohexylcarbodiimide (DCCD; Zhen et al., 1997b); the cytosolically disposed residue (Cys-668 in AVP2; Cys-634 in AVP1), whose alkylation by maleimides irreversibly abolishes catalytic activity (Zhen et al., 1994b; Kim et al., 1995); and both of the sequences (TK[AG]ADVGADLVGK[IV]E and HKAAV[TI]GDT[IV]GDP[LF]K), located in cytosolic loops III and VIII, respectively, that are recognized by the peptide-specific antibodies PAB_{TK} and PAB_{HK} (Kim et al., 1994a; Fig. 1).

The one discernible exception to the conservation of seemingly critical residues was the substitution of an acidic residue at position 441 of AVP2 by Lys and the substitution of Ser at position 445 by an Asp (Fig. 1). The span-loop motif bounding these residues, which in all previously sequenced V-PPases is T[ED]YYTS, was SKYYTD in AVP2. A Glu (or Asp)-to-Lys substitution at this position in AVP2 was surprising because the results of site-directed mutagenesis experiments on AVP1 indicate that an acidic residue in the equivalent position (residue 427) is required for the efficient coupling of PPi hydrolysis to H^+ translocation (Zhen et al., 1997b).

Expression of *AVP2* in Arabidopsis

Northern analyses of total RNA extracted from roots and leaves of Arabidopsis yielded a single 2.6-kb band of approximately equivalent intensity when the blots were hybridized with *AVP2* cDNA (Fig. 2). A similarly abundant 2.4-kb band was detected when the same blots were hybridized with *AVP1* cDNA (Fig. 2). On the basis of these analyses, and on the finding that the *AVP2* and *AVP1* probes did not cross-hybridize on Arabidopsis genomic

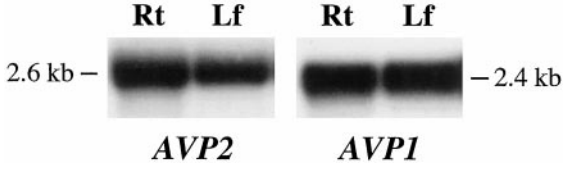

Figure 2. Northern analysis of steady-state levels of *AVP2* and *AVP1* transcripts in leaves (Lf) and roots (Rt) of Arabidopsis. The 2.6- and 2.4-kb bands shown were the only bands detected after hybridization of the blots with *AVP2* or *AVP1* cDNA, respectively.

Southern blots, the steady-state levels of *AVP2* and *AVP1* transcripts were inferred to be similar in the intact plant.

Heterologous Expression of AVP2

The properties of heterologously expressed AVP2 were investigated to determine if, despite its sequence divergence, its functional properties approximated those of AVP1. For this purpose, *Saccharomyces cerevisiae* strain BJ5459 was transformed with vector pYES2 containing the entire coding sequence of *AVP2* (pYES2-AVP) or, for comparisons with membranes lacking V-PPase or containing AVP1, with empty vector (pYES2) or pYES2-AVP1.

High levels of AVP2 expression were achieved by this approach. Vacuolar membrane-enriched vesicles purified from pYES2-AVP2-transformed (BJ5459/pYES2-AVP2) cells contained an intense PAB_{HK}- (and PAB_{TK}-) reactive M_r 67,000 band after SDS-PAGE and western analysis that was absent from the corresponding fraction from untransformed or empty vector control BJ5459 cells (Fig. 3). Furthermore, AVP2 appeared to be expressed and undergo membrane insertion at an efficiency comparable to that of AVP1. The M_r 67,000 polypeptides in the vacuolar membrane-enriched fractions from BJ5459/pYES2-AVP2 and BJ5459/pYES2-AVP1 cells, which were absent from the same cells after transformation with empty vector, reacted with antibody PAB_{HK} with similar intensities (Fig. 3). As noted consistently in previous investigations of endogenous and heterologous V-PPases (Zhen et al., 1997a), AVP2, like AVP1, migrated at a lower M_r value than predicted from its computed mass. This was attributed to anomalous electrophoretic properties associated with the extreme hydrophobicity of all known V-PPases (Zhen et al., 1997a).

AVP2-Catalyzed PPi Hydrolysis

The PAB_{HK}-reactive polypeptide detected in the vacuolar membrane-enriched fraction from BJ5459/pYES2-AVP2 cells was active in PPi hydrolysis. When assayed in reaction buffer containing 250 μM NaF to abolish any contribution from contaminating yeast soluble PPase (Kim et al., 1994a), the kinetics of AVP2-catalyzed PPi hydrolysis were indistinguishable from those of AVP1. The K_m values, PPi concentrations required for maximal activity, and maximal activities of AVP2 and AVP1 were 90 and 110 μM total PPi, 0.3 mM total PPi, and 0.4 to 0.7 and 0.4 to 0.6 μmol mg^{-1}, respectively, at a total Mg^{2+} concentration of 1.3 mM (data not shown). Despite this basic equivalence in the kinetics of PPi hydrolysis, further experiments revealed a marked difference between the two enzymes in terms of their monovalent cation requirements.

AVP2 and AVP1 shared an obligate requirement for Mg^{2+} for activity, but were differentially responsive to monovalent cations. Omission of Mg^{2+} from the reaction medium largely abolished AVP2- and AVP1-mediated PPi hydrolysis, and in neither case could Mn^{2+}, Zn^{2+}, and Ca^{2+} substitute for Mg^{2+} (Fig. 4A). However, in direct contrast to AVP1, whose activity was increased 8-fold by the inclusion of 50 mM KCl or NH_4Cl in the assay medium, AVP2 was not activated by K^+ or any of the other monovalent cations tested (Fig. 4B). Although PPi hydrolysis by some AVP2 preparations showed weak stimulation by monovalent cations, this effect was not K^+-specific.

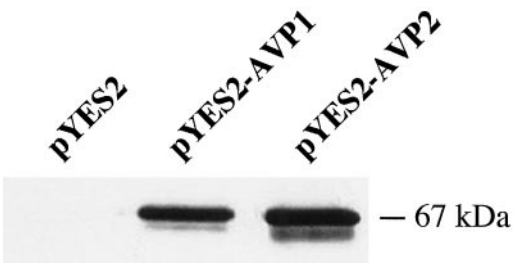

Figure 3. Western analysis of antibody PAB_{HK}-reactive polypeptides in vacuolar membrane-enriched vesicles from pYES2-AVP2-, pYES2-AVP1-, or pYES2-transformed *S. cerevisiae* BJ5459 cells. All lanes were loaded with 5 μg of membrane protein. The M_r 67,000 bands shown were the only immunoreactive species detected.

AVP2-Catalyzed H^+ Translocation

The differential sensitivities of AVP2 and AVP1 to monovalent cations were also evident at the transport level. Heterologously expressed AVP2 was not only competent in PPi hydrolysis, but also in PPi-dependent H^+ translocation, and neither was dependent on the provision of K^+ (Fig. 5). Indeed, AVP2 was capable of mediating higher rates and extents of intravesicular acidification in media containing choline chloride than in media containing KCl. Substitution of the permeant anion Cl^- with the less permeant anion SO_4^{2-} and the impermeant anion gluconate decreased the extent of intravesicular acidification by 20% and 28%, respectively, whereas substitution of K^+ with choline increased the extent of intravesicular acidification by 56% (Fig. 5). In strict contrast, intravesicular acidification by AVP1 was almost completely dependent on K^+. Although AVP1-catalyzed H^+ translocation showed a dependence on anions similar to that of AVP2, intravesicular acidification was negligible when K^+ was substituted by choline (Fig. 5).

Inhibition by Aminomethylenediphosphonate (AMDP) and Ca^{2+}

AVP2 and AVP1 were similarly sensitive to inhibition by the 1,1-diphosphonate AMDP (Zhen et al., 1994a) but differentially sensitive to inhibition by Ca^{2+} (Fig. 6). While the concentration dependencies

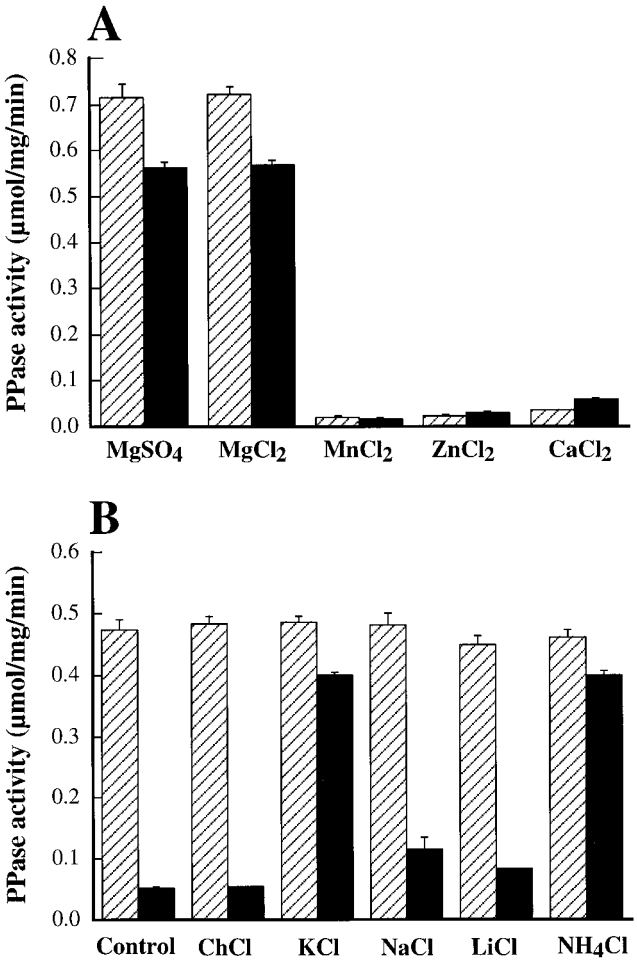

Figure 4. Inorganic cation dependence of PPi hydrolysis by AVP2 (hatched bars) and AVP1 (black bars). A, Divalent cations. B, Monovalent cations. PPi hydrolysis by vacuolar membrane-enriched vesicles (3–5 μg of membrane protein) from pYES2-AVP2 and pYES2-AVP1-transformed *S. cerevisiae* BJ5459 cells was measured in reaction media (300 μL) containing 1.3 mM concentrations of the divalent cations indicated plus 50 mM KCl (A) or 50 mM concentrations of the monovalent cations indicated plus 1.3 mM $MgSO_4$ (B). Control activities were measured in the absence of divalent cation (A) or monovalent cation (B). Values shown are means ± SE (n = 4).

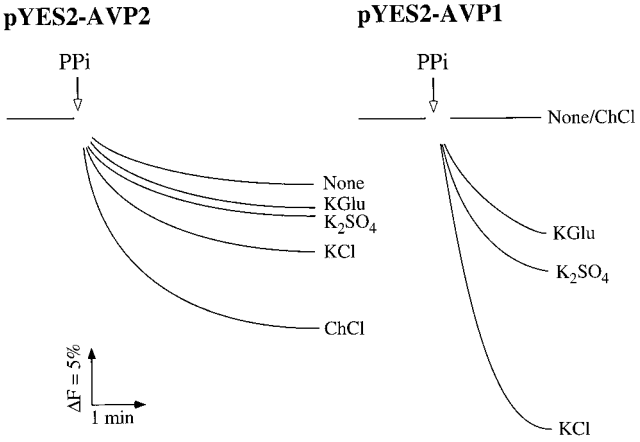

Figure 5. PPi-dependent H^+ translocation by vacuole-enriched membrane fractions from pYES2-AVP2- and pYES2-AVP1-transformed *S. cerevisiae* BJ5459. Intravesicular acidification was monitored with acridine orange in media containing membranes (80 μg of membrane protein), $MgSO_4$ (1.3 mM), and no additional monovalent cations (None), KCl (100 mM), K_2SO_4 (50 mM), K-gluconate (K-Glu, 100 mM), or choline chloride (ChCl, 100 mM). At the times indicated, H^+ translocation was initiated by the addition of imidazole-PPi (0.3 mM). ΔF%, Percentage change in fluorescence.

for inhibition of AVP2- and AVP1-mediated PPi hydrolysis by the type-specific V-PPase inhibitor AMDP superimposed to yield I_{50} values of 0.9 and 1.5 μM, respectively (Fig. 6A), AVP2 was more than 3-fold more sensitive to inhibition by free Ca^{2+} than AVP1 (Fig. 6B). Ca^{2+} at a total concentration of 7.5 μM or a free concentration of 0.5μM, was sufficient to inhibit AVP2-mediated PPi hydrolysis by 50%, whereas concentrations of greater than 50 and 1.7 μM, respectively, were necessary to inhibit AVP1 to the same extent (Fig. 6B).

DISCUSSION

The experiments described establish that *AVP2* encodes a structurally and functionally divergent V-PPase competent in both PPi hydrolysis and PPi-energized H^+-translocation after heterologous expression in *S. cerevisiae*. In direct contrast to AVP1, which has a near obligatory requirement for K^+ for activity and is only moderately sensitive to inhibition by Ca^{2+}, AVP2 is insensitive to K^+ but highly sensitive to Ca^{2+}. It therefore appears that plants contain two categories of V-PPases: prototypical, K^+-activated, AVP1-like (type I) V-PPases and K^+-insensitive, AVP2-like (type II) V-PPases.

To our knowledge, this is the first time that a structural and functional dichotomy of this type has

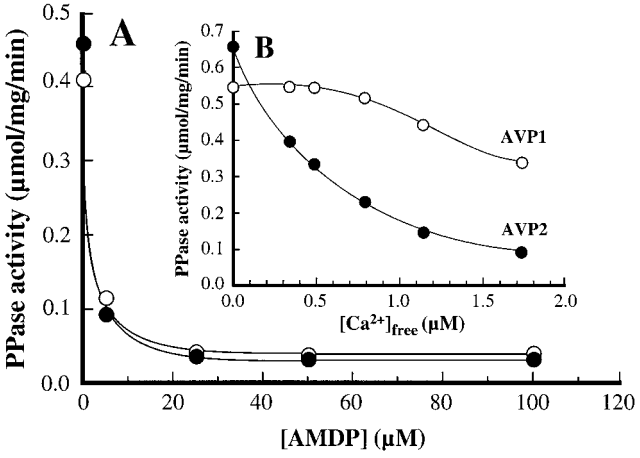

Figure 6. Sensitivities of AVP2- and AVP1-mediated PPi hydrolysis to inhibition by AMDP (A) or Ca^{2+} (B). PPi hydrolysis was measured as described in Figure 4, except that AMDP or Ca^{2+} ($CaCl_2$) was added to achieve the concentrations indicated. Free Ca^{2+} ($[Ca^{2+}]_{free}$) was estimated using the SOLCON program. Values shown are means ± SE (n = 4).

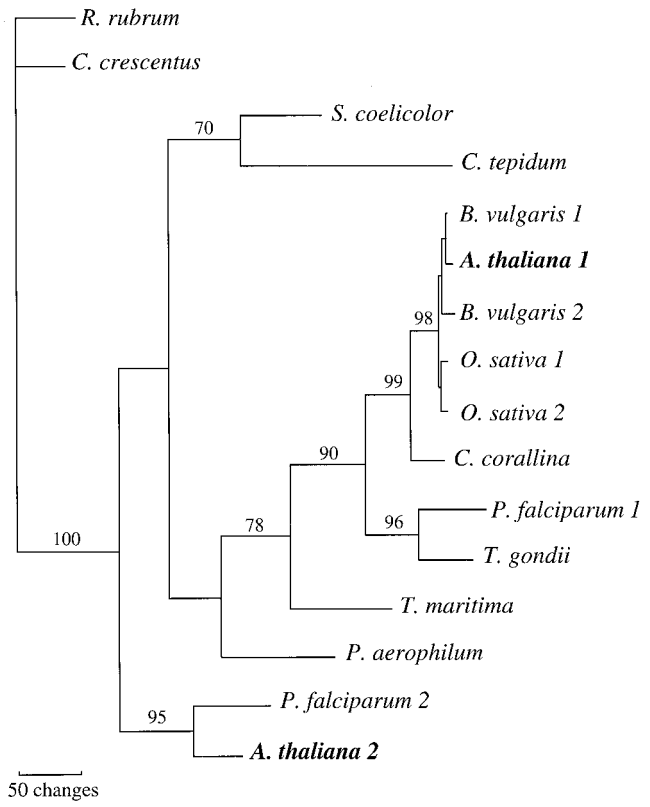

Figure 7. Phylogenetic analysis of V-PPase sequences. V-PPase sequences were aligned using ClustalW 1.7 (Thompson et al., 1994), and the most conserved blocks of sequence (corresponding to positions 161–193, 253–315, 428–496, 571–588, 616–695, 726–752, and 755–798 of AVP2) were subjected to phylogenetic analysis by both maximum parsimony and distance with neighbor-joining methods (PAUP 4.0b2; Saitou and Nei, 1987). Parsimony analysis was performed using a heuristic search of 500 random addition replicates, and both the parsimony and neighbor-joining analyses were subjected to 1,000 bootstrap replicates. Qualitatively similar results were obtained by both procedures, but only the single tree retrieved from parsimony analysis is shown. Bootstrap percentages greater than 50 are indicated above the branches. The sequences shown are those from Arabidopsis (AVP1; GenBank accession no. AB015138; Sarafian et al., 1992), *B. vulgaris* (BVP1 and BVP2; accession nos. AAA61609.1 and AAA61610.1; Kim et al., 1994a), *O. sativa* (OVP1 and OVP2; accession nos. BAA08232 and BAA31524; Sakakibara et al., 1996), *P. falciparum* (accession no. AAD17215), *C. corallina* (accession no. AB018529; Nakanishi et al., 1999), *P. aerophilum* (accession no. AF182812; Drozdowicz et al., 1999), *R. rubrum* (accession no. AAC38615.1; Baltscheffsky et al., 1998), *Streptomyces coelicolor* (accession no. CAB38484), and *Thermotoga maritima* (accession no. AE001702; Nelson et al., 1999). The sequences from *Caulobacter crescentus* (contig gcc 492), and *Chlorobium tepidum* (contig gct 12) were identified by BLAST searches of preliminary sequence data collated by The Institute for Genomic Research (http://www.tigr.org). Sequence 2 from *P. falciparum* was identified by BLAST searches of preliminary data collated by The Institute for Genomic Research, The Sanger Centre (http://www.sanger.ac.uk/projects/p__falciparum), and The Stanford DNA Sequencing and Technology Center (http://www.sequence.stanford.edu/group/malaria). The sequence from *Toxoplasma gondii* was determined by cloning (Y.M. Drozdowicz, B. Striepen, D. Roos, and P.A. Rea, unpublished data).

been defined molecularly for the V-PPases from a single organism. However, reexamination of the available sequence data in the light of what is now known about the functional characteristics of AVP2 indicates that it is probably not an isolated phenomenon. Database searches for V-PPase sequences yielded matches in the archaea, bacteria, and eukaryotes. Phylogenetic analyses of these and previously isolated V-PPase sequences confirm that, rather than being an isoform of AVP1, AVP2 represents a novel category of V-PPase found not only in plants but also in other eukaryotes containing AVP1-like V-PPases. Regardless of the algorithm employed for phylogenetic analysis—maximum parsimony or distance with neighbor-joining methods (Saitou and Nei, 1987)—AVP1 nests deeply within a well-defined lineage of prototypical type I V-PPases consisting of the isoform pairs from beet (*Beta vulgaris*) and rice (*Oryza sativa*), a homolog from *Chara corallina*, and two orthologs from apicomplexan protists (sequence 1 from *P. falciparum* and sequence 1 from *T. gondii*; Fig. 7). AVP2, by contrast, nests within a lineage containing one ortholog from *P. falciparum* (sequence 2) on a branch separate and distinct from the lineage containing AVP1. Two fundamental conclusions therefore follow: (a) while the relationship between the AVP-containing lineages, the archaeal V-PPase, PVP, and the corresponding bacterial sequences have yet to be resolved, AVP2 groups in a manner distinct from that of AVP1 and other type I V-PPases, including their isoforms; (b) in at least one other eukaryotic taxon known to contain V-PPases, the phylum Apicomplexa, an AVP1/AVP2 dichotomy analogous to that of plants is also found.

On the one hand, the presence of V-PPases in the Apicomplexa is consistent with the identification of plant-like (AVP1-like) V-PPase genes and activities in the green algae. Members of the Apicomplexa possess a vestigial, nonphotosynthetic plastid, the apicoplast, which is considered to have arisen from the symbiosis of an algal cell by a proto-Apicomplexan (Kohler et al., 1997). On the other hand, the coexistence in both Arabidopsis and *Plasmodium* of type I and type II V-PPases raises questions regarding the distribution of type II V-PPases among algae and other plastid-containing eukaryotes, including euglenoids, dinoflagellates, cryptomonads, and chlorarachniophytes. Are both of the V-PPase categories found in plants and the Apicomplexa of algal origin, or is one (or both) of more ancient origin?

The isolation and characterization of AVP2 not only demonstrates the diversity of V-PPases between and within organisms, but is also of considerable strategic value for understanding the structure-function relationships of V-PPases. As detailed previously for another idiotypic V-PPase, PVP (Drozdowicz et al., 1999), the overall divergence of the sequence of AVP2 from that of AVP1 and other characterized V-PPases will undoubtedly facilitate the identification of resi-

dues or motifs of mechanistic relevance. In the context of core catalysis, examples include: (a) the fundamental correspondence of the putative topology of AVP2 (with the exception of the N terminus) to that of AVP1 and other V-PPases, suggesting a basic uniformity of secondary structure despite their disparate primary structures; (b) retention in AVP2 of the same four regions that are subject to stringent conservation in AVP1, PVP, and RVP (Drozdowicz et al., 1999)—the putative core catalytic cytosolic loop III, which encompasses both the universal PPase consensus motif DX_7KXE (Rea et al., 1992b) and the antibody PAB_{TK}-reactive sequence (Kim et al., 1994a), positions 532 to 548 located in cytosolic loop VI, and positions 737 to 748 and 760 to 772, the latter of which coincides with the antibody PAB_{HK}-reactive sequence in the C-terminal tail; (c) conservation of residues Glu-323 and Asp-532, and residue Cys-668, whose equivalents in AVP1 (Glu-305 and Asp-504, and Cys-634) confer DCCD sensitivity (Zhen et al., 1997b) and reactivity and substrate-protectable sensitivity, respectively, toward both membrane-permeant and -impermeant maleimides (Zhen et al., 1994b; Kim et al., 1995).

A surprising feature of AVP2 that may eventually provide insight into the specific events underlying core catalysis is the replacement of the otherwise V-PPase-conserved motif T[DE]YYTS by the sequence SKYYTD at the span-loop interface of cytosolic loop V. Since the equivalent of this motif in AVP1 encompasses the acidic residue (Glu-427) inferred to participate in coupling PPi hydrolysis to H^+ translocation (Zhen et al., 1997b), it might be expected that, as in AVP1 E427Q mutants (Zhen et al., 1997b), a Lys substitution at this position would result in an enzyme defective in H^+ translocation. However, this is clearly not the case: heterologously expressed AVP2 is active in PPi-energized H^+ translocation. Moreover, AVP2's cognate from *P. falciparum* (Fig. 7) possesses a similarly substituted sequence (TRYYTD) at the same position, suggesting that the sequence T[acidic]YYT[neutral] is specific to type I V-PPases, while the sequence T[basic]YYT[acidic] is specific to type II V-PPases. Therefore, in the context of mechanism, two conclusions can be made: (a) AVP1 Glu-427 does not directly participate in H^+ translocation, which seems unlikely in view of the enhanced capacity of AVP1 E427D mutants for H^+ translocation (Zhen et al., 1997b); or (b) AVP2 (and, by implication, the *P. falciparum* type II enzyme) is competent in H^+ translocation because a second substitution (Ser to Asp) three places displaced from this position introduces an acidic residue that can serve the same function as Glu-427 (or an Asp-427).

With regard to type-specific functions, AVP2's insensitivity to K^+ and its pronounced sensitivity to inhibition by Ca^{2+} offer the means for delineating the structural basis of these properties. Specifically, given the facility with which both AVP2 and AVP1 can be expressed at high levels in a transport-active state in *S. cerevisiae*, it should now be practicable to delimit those portions of AVP1 and AVP2 involved in sensing K^+ and Ca^{2+} and in modulating activity in response to these ligands by the functional analysis of AVP1/AVP2 chimeras.

The most immediate research priority for AVP2 and other type II V-PPases is to determine their subcellular localization. Candidates include the plasma, Golgi, mitochondrial, and chloroplast membranes, as well as the vacuolar membrane itself. Although the predominant PPase activities on the vacuolar, Golgi, and plasma membranes are K^+-dependent (AVP1-like; Chanson et al., 1985; Long et al., 1997; Ratajczak et al., 1999), the possibility that K^+-independent (AVP2-like) V-PPases are also co-resident on one or more of these membranes cannot be excluded completely. Type II V-PPases may have a restricted tissue distribution compared with their type I counterparts. Likewise, the possibility that AVP2 and AVP1 represent individual α- and β-subunits of a vacuolar V-PPase heteromultimer is not necessarily refuted by the sufficiency of heterologously expressed AVP2 and AVP1 for core catalysis. Individual subunits and/or α-α or β-β homomultimers are sufficient for catalysis, but it is not known if the properties of enzyme constituted of α-β heteromultimers might better simulate those of the in vivo complex.

The possibility of a mitochondrial or chloroplast membrane localization for AVP2—one consistent with the abundance of *AVP2* transcripts in both roots and leaves—will necessitate critical reevaluation of the status of PPases in these organelles and the generation of AVP2-specific and AVP1-specific antibodies. In the case of the mitochondrial enzyme, it has yet to be determined unequivocally if the activities measured are specifically associated with the inner mitochondrial membrane, or if they represent contamination of this fraction with vacuolar membrane vesicles. The kinetics, inhibitor sensitivities, and monovalent cation requirements of the putative mitochondrial enzyme from pea (Vianello et al., 1991), the most thoroughly characterized to date, are remarkably similar to those of most AVP1-type V-PPases. Moreover, despite claims that vacuolar membrane contamination is low in these preparations, there is a bias against the identification of such contaminants inherent in the procedures used.

Although most of the ATP-dependent H^+ translocation measured is sensitive to oligomycin rather than to bafilomycin A_1, suggesting a predominantly mitochondrial origin, the validity of this conclusion is compromised because the submitochondrial particles used were derived from mitochondria suspended in ice-cold media containing millimolar concentrations of ATP (Vianello et al., 1991; Zancani et al., 1995). These conditions are known to result in appreciable cold-inactivation of V-ATPases (Parry et al., 1989) and lead to gross underestimates of vacuo-

lar membrane contamination when bafilomycin A_1-sensitive ATPase activity is the sole criterion used to assess such contamination. Similarly problematic is the finding that the properties of the putative catalytic subunit of the mitochondrial H^+-PPase better approximate those of canonical eukaryotic soluble PPases in terms of size (approximately 35 kD), hydrophilicity, and catalytic activity (Cooperman et al., 1992) than those of the SMPs from which the purified product was derived (Zancani et al., 1995). In the case of the membrane-associated PPase of plastids, the situation seems better defined insofar as this enzyme has the same basic properties before and after purification and an apparent subunit size after SDS-PAGE of 55 kD, but it remains to be determined if this moiety is competent in PPi-energized H^+ translocation (Jiang et al., 1997).

One hypothesis that will be explored, particularly if AVP2 is found to localize to mitochondrial or plastid membranes and have a H^+:PPi stoichiometry of 2 or greater, is that this category of V-PPase augments the cytosolic PPi pool by catalyzing redox-coupled PPi synthesis. Preliminary estimates of the H^+:PPi stoichiometry of the putative mitochondrial enzyme are consistent with a value of 2 (Zancani et al., 1995). Pending corroboration—specifically, tests of the capacity of SMPs for net H^+-gradient-energized PPi synthesis from Pi—such stoichiometric ratios might mean that PPi is synthesized in mitochondria by a V-PPase-like enzyme (possibly an AVP2-like V-PPase) and is then exported to the cytosol for utilization by AVP1-like V-PPases and other PPi-dependent enzymes, including PPi:phosphofructokinase and UDP-Glc pyrophosphorylase. Indications of the facility of the inner mitochondrial membrane for PPi/ADP exchange are at least consistent with this proposal, and the fascinating possibility that, in the same way as F-ATPases (whether mitochondrial or chloroplastic) provide ATP for paralogous V-ATPases, type II V-PPases may provide PPi for paralogous type I V-PPases.

MATERIALS AND METHODS

Plant Materials

Arabidopsis cv Columbia was used throughout. Total RNA was isolated from roots and leaves of 21-d-old seedlings grown in Gamborg's B-5 liquid medium using a RNEasy kit (Qiagen USA, Valencia, CA) according to the manufacturer's specifications.

Isolation of *AVP2*

The coding sequence of *AVP2* was amplified by reverse transcription-PCR of Arabidopsis leaf total RNA. First-strand synthesis was performed using a pre-amplification system (Superscript II, Life Technologies, Grand Island, NY). PCR was performed with *Pfu* DNA polymerase (Stratagene, La Jolla, CA) using 5′ and 3′ primers corresponding to positions 1 through 20 and 2,299 through 2,322, respectively, of the cDNA predicted from the genomic sequence of *AVP2* (GenBank accession no. AC005679). An *Xba*I restriction site was engineered into the 3′ primer to facilitate cloning. For functional characterization of AVP2 after heterologous expression in *Saccharomyces cerevisiae*, the resulting 2.4-kb PCR product was restricted with *Xba*I and subcloned into the multicloning site of *Pvu*II-*Xba*I double-digested pYES2 expression vector (Invitrogen, Carlsbad, CA) to generate pYES2-AVP2. The fidelity of the amplified sequence of *AVP2* was determined by dye terminator chemistry using nested oligonucleotide primers. Plasmid pYES2-AVP1, containing the coding sequence of *AVP1*, was constructed as described previously (Kim et al., 1994a).

Heterologous Expression in Yeast

Vacuolar protease-deficient *S. cerevisiae* strain BJ5459 (*Mat*α, *ura3-52*, *trp1*, *lys2-801*, *leu2*Δ*1*, *his3-*Δ*200*, *pep4::HIS3*, *prb*Δ*1.6R*, *can1*, and *GAL*) transformants containing empty vector (pYES2), pYES2-AVP2, or pYES2-AVP1 were generated by the LiOAc/PEG method, selected for uracil prototrophy, and subjected to membrane fractionation as described previously (Kim et al., 1994a; Zhen et al., 1997b; Drozdowicz et al., 1999).

Measurement of PPi Hydrolysis and H^+-Translocation

PPi hydrolytic activity was assayed as described previously (Zhen et al., 1997b) except that imidazole-based rather than Tris- or Bis-Tris-propane-based buffers were used throughout to preclude competition with K^+ and other monovalent cations (Gordon-Weeks et al., 1997). PPase activities are expressed as micromoles of PPi hydrolyzed per milligram of protein per minute. PPi-dependent intravesicular acidification was monitored fluorimetrically using acridine orange (2.5 μM) as an indicator, as described previously (Zhen et al., 1997b).

Northern and Western Analyses

For northern analyses, samples of total RNA (10 μg) were electrophoresed on 10% (v/v) formaldehyde-agarose gels and transferred to Hybond-N membrane filters (Amersham Pharmacia Biotech, Buckinghamshire, UK). The blots were hybridized in 7% (w/v) SDS, 1 mM EDTA, and 0.3 M sodium phosphate buffer, pH 7.2, containing ^{32}P-labeled random-primed probes corresponding to the coding sequences of *AVP2* or *AVP1* (Sarafian et al., 1992). For western analyses of AVP2 and AVP1 after heterologous expression in yeast, vacuolar membrane-enriched vesicles were subjected to denaturation, SDS-PAGE, electrotransfer, and immunoreaction with the antibodies PAB_{HK} or PAB_{TK}, as described previously (Zhen et al., 1997b). Immunoreactive bands were visualized by enhanced chemiluminescence (Amersham Pharmacia Biotech).

Protein Estimations

Protein was estimated by the method of Bradford (1976).

Computer Programs

For measurements of the susceptibility of V-PPase activity to inhibition by Ca^{2+}, the concentration of free Ca^{2+} ($[Ca^{2+}]_{free}$) was estimated by substitution of the appropriate stability constants into the SOLCON program (a gift from Dr. Yale Goldman, University of Pennsylvania). The stability constants were obtained from Martell and Smith (1974) and Smith and Martell (1976) and deployed as described previously (Rea et al., 1992a). Sequences were aligned using ClustalW 1.7 (Thompson et al., 1994). The putative membrane topology of AVP2 was modeled using TopPred II version 1.3 (Claros and von Heijne, 1994), as described for AVP1 (Zhen et al., 1997) and PVP (Drozdowicz et al., 1999.) Phylogenetic analyses were performed using maximum parsimony and the neighbor-joining methods of the PAUP 4.0b1 software package (Phylogenetic Analysis Using Parsimony [*and Other Methods], version 4.02b. Sinauer Associates, Sunderland, MA; Saitou and Nei, 1987).

NOTE ADDED IN PROOF

The cloning of the *AVP2* cDNA has also been reported by Nakanishi and Maeshima (Nakanishi Y, Maeshima M [2000] Isolation of a cDNA for a H^+-pyrophosphatase-like protein from Arabidopsis [accession no. AB034696] and its functional expression in yeast [PGR 00–026]. Plant Physiol **122:** 985).

ACKNOWLEDGMENT

We thank Dr. Yale Goldman, Department of Physiology, University of Pennsylvania, for the kind gift of the SOLCON program.

Received November 1, 1999; accepted January 25, 2000.

LITERATURE CITED

Baltscheffsky H (1996) Energy conversion leading to the origin and early evolution of life: did inorganic pyrophosphate precede adenosine triphosphate? *In* H Baltscheffsky, ed, Origin and Evolution of Biological Energy Conversion. VCH Publishers, New York, pp 1–9

Baltscheffsky M, Nadanaciva S, Schultz A (1998) A pyrophosphate synthase gene: molecular cloning and sequencing of the cDNA encoding the inorganic pyrophosphate synthase from *Rhodospirillum rubrum*. Biochim Biophys Acta **1364:** 301–306

Bradford MM (1976) A rapid and sensitive method for the quantitation of microgram quantities of protein utilizing the principle of protein-dye binding. Anal Biochem **72:** 248–254

Britten CJ, Zhen RG, Kim EJ, Rea PA (1992) Reconstitution of transport function of vacuolar H^+-translocating inorganic pyrophosphatase. J Biol Chem **267:** 21850–21855

Chanson A, Fichmann J, Spear D, Taiz L (1985) Pyrophosphate-driven proton transport by microsomal membranes of corn coleoptiles. Plant Physiol **79:** 159–164

Claros MG, von Heijne G (1994) TopPred II: an improved software for membrane protein structure predictions. Comput Appl Biosci **10:** 685–686

Cooperman BS, Baykov AA, Lahti R (1992) Evolutionary conservation of the active site of soluble inorganic pyrophosphatase. Trends Biochem Sci **17:** 262–266

Davies JM, Rea PA, Sanders D (1991) Vacuolar proton-pumping pyrophosphatase in *Beta vulgaris* shows vectorial activation by potassium. FEBS Lett **278:** 66–68

Drozdowicz YM, Lu YP, Patel V, Fitz-Gibbon S, Miller JH, Rea PA (1999) A thermostable vacuolar-type membrane pyrophosphatase from the archaeon *Pyrobaculum aerophilum*: implications for the origins of pyrophosphate-energized pumps. FEBS Lett **460:** 505–512

Gordon-Weeks R, Korenkov VD, Steele SH, Leigh RA (1997) Tris is a competitive inhibitor of K^+ activation of the vacuolar H^+-pumping pyrophosphatase. Plant Physiol **114:** 901–905

Hartmann E, Rapoport TA, Lodish HF (1989) Predicting the orientation of eukaryotic membrane-spanning proteins. Proc Natl Acad Sci USA **89:** 5786–5790

Jiang SS, Fan LL, Yang SJ, Kuo SY, Pan RL (1997) Purification and characterization of thylakoid membrane-bound inorganic pyrophosphatase from *Spinacia oleracia* L. Arch Biochem Biophys **346:** 105–112

Kim EJ, Zhen RG, Rea PA (1994a) Heterologous expression of plant vacuolar pyrophosphatase in yeast demonstrates sufficiency of the substrate-binding subunit for proton transport. Proc Natl Acad Sci USA **91:** 6128–6132

Kim EJ, Zhen RG, Rea PA (1995) Site-directed mutagenesis of vacuolar H^+-pyrophosphatase: necessity of Cys^{634} for inhibition by maleimides but not catalysis. J Biol Chem **270:** 2630–2635

Kim Y, Kim EJ, Rea PA (1994b) Isolation and characterization of cDNAs encoding the vacuolar H^+-pyrophosphatase of *Beta vulgaris*. Plant Physiol **106:** 375–382

Kohler S, Delwiche CF, Denny PW, Tilney LG, Webster P, Wilson RJ, Palmer JD, Roos DS (1997) A plastid of probable green algal origin in Apicomplexan parasites. Science **275:** 1485–1489

Long AR, Hall JL, Williams LE (1997) Chromatographic resolution, purification, and characterization of H^+-PPase and H^+-ATPase from *Ricinus* cotyledons. J Plant Physiol **151:** 16–24

Martell AE, Smith RM (1974) Critical Stability Constants, Vol 1. Plenum Press, New York

Nakanishi Y, Matsuda N, Aizawa K, Kashiyama T, Yamamoto K, Mimura T, Ikeda M, Maeshima M (1999) Molecular cloning and sequencing of the cDNA for vacuolar H^+-pyrophosphatase from *Chara corallina*. Biochim Biophys Acta **1418:** 245–250

Nelson KE, Clayton RA, Gill SR, Gwinn ML, Dodson RJ, Haft DH, Hickey EK, Peterson JD, Nelson WC, Ketchum KA, McDonald L, Utterback TR, Malek JA, Linher KD, Garrett MM, Stewart AM, Cotton MD, Pratt MS, Phillips CA, Richardson D, Heidelberg J, Sutton GG, Fleischmann RD, Eisen JA, Fraser CM (1999) Evidence for lateral gene transfer between archaea and bacteria from genome sequence of *Thermotoga maritima*. Nature **399:** 323–329

Nyren P, Strid A (1991) Hypothesis: the physiological role of the membrane-bound proton-translocating pyrophosphatase in some phototrophic bacteria. FEBS Lett **77:** 265–270

Parry RV, Turner JC, Rea PA (1989) High purity preparations of higher plant vacuolar H^+-ATPase reveal additional subunits: revised subunit composition. J Biol Chem **264:** 20025–20032

Ratajczak R, Hinz G, Robinson DG (1999) Localization of pyrophosphatase in membranes of cauliflower inflorescence cells. Planta **208:** 215–211

Rea PA, Britten CJ, Jennings IR, Calvert CM, Skiera LA, Leigh RA, Sanders D (1992a) Regulation of vacuolar H^+-pyrophosphatase by free calcium: a reaction kinetic analysis. Plant Physiol **100:** 1706–1715

Rea PA, Kim Y, Sarafian V, Poole RJ, Davies JM, Sanders D (1992b) Vacuolar H^+-translocating pyrophosphatases: a new category of ion translocase. Trends Biochem Sci **17:** 348–353

Rea PA, Poole RJ (1993) Vacuolar H^+-translocating pyrophosphatase. Annu Rev Plant Physiol Plant Mol Biol **44:** 157–180

Rodrigues CO, Scott DA, Docampo R (1999) Presence of a vacuolar H^+-pyrophosphatase in promastigotes of *Leishmania donovani* and its localization to a different compartment from the vacuolar H^+-ATPase. Biochem J **340:** 759–766

Saitou N, Nei M (1987) The neighbor-joining method: a new method for reconstructing phylogenetic trees. Mol Biol Evol **4:** 406–425

Sakakibara Y, Kobayashi H, Kasamo K (1996) Isolation and characterization of cDNAs encoding vacuolar H^+-pyrophosphatase isoforms from rice (*Oryza sativa* L.). Plant Mol Biol **31:** 1029–1038

Sarafian V, Kim Y, Poole RJ, Rea PA (1992) Molecular cloning and sequence of cDNA encoding the pyrophosphate-energized vacuolar membrane proton pump of *Arabidopsis thaliana*. Proc Natl Acad Sci USA **89:** 1775–1779

Sato MH, Kasahara M, Ishii N, Homareda H, Matsui H, Yoshida M (1994) Purified vacuolar inorganic pyrophosphatase consisting of a 75-kDa polypeptide can pump H^+ into reconstituted proteoliposomes. J Biol Chem **269:** 6725–6728

Scott DA, de Souza W, Benchimol M, Zhong L, Lu HG, Moreno SN, Docampo R (1998) Presence of a plant-like proton-pumping pyrophosphatase in acidocalcisomes of *Trypanosoma cruzi*. J Biol Chem **273:** 22151–22158

Smith RM, Martell AE (1976) Critical Stability Constants, Vol 4. Plenum Press, New York

Thompson JD, Higgins DG, Gibson TJ (1994) CLUSTAL W: improving the sensitivity of progressive multiple sequence alignment through sequence weighting, position-specific gap penalties and weight matrix choice. Nucleic Acids Res **22:** 4673–4680

Vianello A, Zancani M, Braidot E, Petrussa E, Macri F (1991) Proton pumping inorganic pyrophosphatase of pea stem submitochondrial particles. Biochim Biophys Acta **1060:** 299–302

von Heijne G (1986) The distribution of positively charged residues in bacterial inner membrane proteins correlates with transmembrane topology. EMBO J **5:** 3021–3027

von Heijne G (1992) Membrane protein structure prediction: hydrophobicity analysis and the positive-inside rule. J Mol Biol **225:** 487–494

Zancani M, Macri F, Dal Belin Peruffo A, Vianello A (1995) Isolation of the catalytic subunit of a membrane-bound H^+-pyrophosphatase from pea stem mitochondria. Eur J Biochem **228:** 138–143

Zhen RG, Baykov AA, Bakuleva NP, Rea PA (1994a) Aminomethylenediphosphonate: a potent type-specific inhibitor of both plant and phototrophic bacterial H^+-pyrophosphatases. Plant Physiol **104:** 153–159

Zhen RG, Kim EJ, Rea PA (1994b) Localization of cytosolically oriented maleimide-reactive domain of vacuolar H^+-pyrophosphatase. J Biol Chem **269:** 23342–23350

Zhen RG, Kim EJ, Rea PA (1997a) The molecular and biochemical basis of pyrophosphate-energized proton translocation at the vacuolar membrane. Adv Bot Res **25:** 297–337

Zhen RG, Kim EJ, Rea PA (1997b) Acidic residues necessary for pyrophosphate-energized pumping and inhibition of the vacuolar H^+-pyrophosphatase by *N,N′*-dicyclohexylcarbodiimide. J Biol Chem **272:** 22340–22348